Evidence for the decay $\Omega_c^0 \to \pi^+\Omega(2012)^- \to \pi^+(\bar{K}\Xi)^-$

Y. Li,[11] S. S. Tang,[11] S. Jia,[11] C. P. Shen,[11] I. Adachi,[17,13] H. Aihara,[81] S. Al Said,[75,35] D. M. Asner,[3] H. Atmacan,[7] V. Aulchenko,[4,62] T. Aushev,[19] R. Ayad,[75] V. Babu,[8] S. Bahinipati,[22] P. Behera,[24] M. Bessner,[16] T. Bilka,[5] J. Biswal,[33] A. Bozek,[59] M. Bračko,[48,33] P. Branchini,[30] T. E. Browder,[16] A. Budano,[30] M. Campajola,[29,54] D. Červenkov,[5] M.-C. Chang,[10] P. Chang,[58] V. Chekelian,[49] A. Chen,[56] B. G. Cheon,[15] K. Chilikin,[42] H. E. Cho,[15] K. Cho,[37] S.-J. Cho,[87] Y. Choi,[73] S. Choudhury,[23] D. Cinabro,[85] S. Cunliffe,[8] S. Das,[47] N. Dash,[24] G. De Nardo,[29,54] G. De Pietro,[30] F. Di Capua,[29,54] Z. Doležal,[5] T. V. Dong,[11] D. Epifanov,[4,62] T. Ferber,[8] B. G. Fulsom,[64] R. Garg,[65] V. Gaur,[84] A. Giri,[23] P. Goldenzweig,[34] B. Golob,[44,33] E. Graziani,[30] T. Gu,[66] K. Gudkova,[4,62] C. Hadjivasiliou,[64] S. Halder,[76] K. Hayasaka,[61] H. Hayashii,[55] W.-S. Hou,[58] K. Inami,[53] A. Ishikawa,[17,13] M. Iwasaki,[63] Y. Iwasaki,[17] W. W. Jacobs,[25] E.-J. Jang,[14] Y. Jin,[81] K. K. Joo,[6] K. H. Kang,[40] G. Karyan,[8] C. Kiesling,[49] C. H. Kim,[15] D. Y. Kim,[72] K.-H. Kim,[87] S. H. Kim,[70] Y.-K. Kim,[87] K. Kinoshita,[7] P. Kodyš,[5] T. Konno,[36] A. Korobov,[4,62] S. Korpar,[48,33] E. Kovalenko,[4,62] P. Križan,[44,33] R. Kroeger,[50] P. Krokovny,[4,62] T. Kuhr,[45] M. Kumar,[47] K. Kumara,[85] A. Kuzmin,[4,62] Y.-J. Kwon,[87] K. Lalwani,[47] M. Laurenza,[30,88] S. C. Lee,[40] C. H. Li,[43] L. K. Li,[7] L. Li Gioi,[49] J. Libby,[24] K. Lieret,[45] D. Liventsev,[85,17] M. Masuda,[80,67] T. Matsuda,[51] D. Matvienko,[4,62,42] J. T. McNeil,[9] M. Merola,[29,54] K. Miyabayashi,[55] R. Mizuk,[42,19] G. B. Mohanty,[76] T. Mori,[53] R. Mussa,[31] M. Nakao,[17,13] Z. Natkaniec,[59] A. Natochii,[16] L. Nayak,[23] M. Nayak,[78] M. Niiyama,[39] N. K. Nisar,[3] S. Nishida,[17,13] K. Nishimura,[16] H. Ono,[60,61] Y. Onuki,[81] P. Oskin,[42] P. Pakhlov,[42,52] G. Pakhlova,[19,42] S. Pardi,[29] S.-H. Park,[17] A. Passeri,[30] S. Paul,[77,49] T. K. Pedlar,[46] R. Pestotnik,[33] L. E. Piilonen,[84] T. Podobnik,[44,33] V. Popov,[19] E. Prencipe,[20] M. T. Prim,[2] N. Rout,[24] G. Russo,[54] D. Sahoo,[76] Y. Sakai,[17,13] S. Sandilya,[23] A. Sangal,[7] L. Santelj,[44,33] T. Sanuki,[79] V. Savinov,[66] G. Schnell,[1,21] C. Schwanda,[27] Y. Seino,[61] K. Senyo,[86] M. Shapkin,[28] C. Sharma,[47] V. Shebalin,[16] J.-G. Shiu,[58] A. Sokolov,[28] E. Solovieva,[42] M. Starič,[33] Z. S. Stottler,[84] M. Sumihama,[12] T. Sumiyoshi,[83] W. Sutcliffe,[2] M. Takizawa,[71,18,68] K. Tanida,[32] F. Tenchini,[8] K. Trabelsi,[41] M. Uchida,[82] T. Uglov,[42,19] Y. Unno,[15] K. Uno,[61] S. Uno,[17,13] Y. Usov,[4,62] S. E. Vahsen,[16] R. Van Tonder,[2] G. Varner,[16] A. Vinokurova,[4,62] E. Waheed,[17] C. H. Wang,[57] E. Wang,[66] M.-Z. Wang,[58] P. Wang,[26] S. Watanuki,[41] O. Werbycka,[59] E. Won,[38] B. D. Yabsley,[74] W. Yan,[69] S. B. Yang,[38] H. Ye,[8] J. Yelton,[9] J. H. Yin,[38] C. Z. Yuan,[26] Y. Yusa,[61] Z. P. Zhang,[69] V. Zhilich,[4,62] and V. Zhukova[42]

(Belle Collaboration)

[1]*Department of Physics, University of the Basque Country UPV/EHU, 48080 Bilbao*
[2]*University of Bonn, 53115 Bonn*
[3]*Brookhaven National Laboratory, Upton, New York 11973*
[4]*Budker Institute of Nuclear Physics SB RAS, Novosibirsk 630090*
[5]*Faculty of Mathematics and Physics, Charles University, 121 16 Prague*
[6]*Chonnam National University, Gwangju 61186*
[7]*University of Cincinnati, Cincinnati, Ohio 45221*
[8]*Deutsches Elektronen–Synchrotron, 22607 Hamburg*
[9]*University of Florida, Gainesville, Florida 32611*
[10]*Department of Physics, Fu Jen Catholic University, Taipei 24205*
[11]*Key Laboratory of Nuclear Physics and Ion-beam Application (MOE) and Institute of Modern Physics, Fudan University, Shanghai 200443*
[12]*Gifu University, Gifu 501-1193*
[13]*SOKENDAI (The Graduate University for Advanced Studies), Hayama 240-0193*
[14]*Gyeongsang National University, Jinju 52828*
[15]*Department of Physics and Institute of Natural Sciences, Hanyang University, Seoul 04763*
[16]*University of Hawaii, Honolulu, Hawaii 96822*
[17]*High Energy Accelerator Research Organization (KEK), Tsukuba 305-0801*
[18]*J-PARC Branch, KEK Theory Center, High Energy Accelerator Research Organization (KEK), Tsukuba 305-0801*
[19]*National Research University Higher School of Economics, Moscow 101000*
[20]*Forschungszentrum Jülich, 52425 Jülich*
[21]*IKERBASQUE, Basque Foundation for Science, 48013 Bilbao*
[22]*Indian Institute of Technology Bhubaneswar, Satya Nagar 751007*
[23]*Indian Institute of Technology Hyderabad, Telangana 502285*
[24]*Indian Institute of Technology Madras, Chennai 600036*
[25]*Indiana University, Bloomington, Indiana 47408*

[26]*Institute of High Energy Physics, Chinese Academy of Sciences, Beijing 100049*
[27]*Institute of High Energy Physics, Vienna 1050*
[28]*Institute for High Energy Physics, Protvino 142281*
[29]*INFN—Sezione di Napoli, 80126 Napoli*
[30]*INFN—Sezione di Roma Tre, I-00146 Roma*
[31]*INFN—Sezione di Torino, 10125 Torino*
[32]*Advanced Science Research Center, Japan Atomic Energy Agency, Naka 319-1195*
[33]*J. Stefan Institute, 1000 Ljubljana*
[34]*Institut für Experimentelle Teilchenphysik, Karlsruher Institut für Technologie, 76131 Karlsruhe*
[35]*Department of Physics, Faculty of Science, King Abdulaziz University, Jeddah 21589*
[36]*Kitasato University, Sagamihara 252-0373*
[37]*Korea Institute of Science and Technology Information, Daejeon 34141*
[38]*Korea University, Seoul 02841*
[39]*Kyoto Sangyo University, Kyoto 603-8555*
[40]*Kyungpook National University, Daegu 41566*
[41]*Université Paris-Saclay, CNRS/IN2P3, IJCLab, 91405 Orsay*
[42]*P.N. Lebedev Physical Institute of the Russian Academy of Sciences, Moscow 119991*
[43]*Liaoning Normal University, Dalian 116029*
[44]*Faculty of Mathematics and Physics, University of Ljubljana, 1000 Ljubljana*
[45]*Ludwig Maximilians University, 80539 Munich*
[46]*Luther College, Decorah, Iowa 52101*
[47]*Malaviya National Institute of Technology Jaipur, Jaipur 302017*
[48]*Faculty of Chemistry and Chemical Engineering, University of Maribor, 2000 Maribor*
[49]*Max-Planck-Institut für Physik, 80805 München*
[50]*University of Mississippi, University, Mississippi 38677*
[51]*University of Miyazaki, Miyazaki 889-2192*
[52]*Moscow Physical Engineering Institute, Moscow 115409*
[53]*Graduate School of Science, Nagoya University, Nagoya 464-8602*
[54]*Università di Napoli Federico II, 80126 Napoli*
[55]*Nara Women's University, Nara 630-8506*
[56]*National Central University, Chung-li 32054*
[57]*National United University, Miao Li 36003*
[58]*Department of Physics, National Taiwan University, Taipei 10617*
[59]*H. Niewodniczanski Institute of Nuclear Physics, Krakow 31-342*
[60]*Nippon Dental University, Niigata 951-8580*
[61]*Niigata University, Niigata 950-2181*
[62]*Novosibirsk State University, Novosibirsk 630090*
[63]*Osaka City University, Osaka 558-8585*
[64]*Pacific Northwest National Laboratory, Richland, Washington 99352*
[65]*Panjab University, Chandigarh 160014*
[66]*University of Pittsburgh, Pittsburgh, Pennsylvania 15260*
[67]*Research Center for Nuclear Physics, Osaka University, Osaka 567-0047*
[68]*Meson Science Laboratory, Cluster for Pioneering Research, RIKEN, Saitama 351-0198*
[69]*Department of Modern Physics and State Key Laboratory of Particle Detection and Electronics, University of Science and Technology of China, Hefei 230026*
[70]*Seoul National University, Seoul 08826*
[71]*Showa Pharmaceutical University, Tokyo 194-8543*
[72]*Soongsil University, Seoul 06978*
[73]*Sungkyunkwan University, Suwon 16419*
[74]*School of Physics, University of Sydney, New South Wales 2006*
[75]*Department of Physics, Faculty of Science, University of Tabuk, Tabuk 71451*
[76]*Tata Institute of Fundamental Research, Mumbai 400005*
[77]*Department of Physics, Technische Universität München, 85748 Garching*
[78]*School of Physics and Astronomy, Tel Aviv University, Tel Aviv 69978*
[79]*Department of Physics, Tohoku University, Sendai 980-8578*
[80]*Earthquake Research Institute, University of Tokyo, Tokyo 113-0032*
[81]*Department of Physics, University of Tokyo, Tokyo 113-0033*
[82]*Tokyo Institute of Technology, Tokyo 152-8550*
[83]*Tokyo Metropolitan University, Tokyo 192-0397*
[84]*Virginia Polytechnic Institute and State University, Blacksburg, Virginia 24061*

[85]*Wayne State University, Detroit, Michigan 48202*
[86]*Yamagata University, Yamagata 990-8560*
[87]*Yonsei University, Seoul 03722*
[88]*Dipartimento di Matematica e Fisica, Università di Roma Tre, I-00146 Roma*

(Received 2 June 2021; accepted 27 July 2021; published 10 September 2021)

Using a data sample of 980 fb^{-1} collected with the Belle detector operating at the KEKB asymmetric-energy e^+e^- collider, we present evidence for the $\Omega(2012)^-$ in the resonant substructure of $\Omega_c^0 \to \pi^+(\bar{K}\Xi)^-$ ($(\bar{K}\Xi)^- = K^-\Xi^0 + \bar{K}^0\Xi^-$) decays. The significance of the $\Omega(2012)^-$ signal is 4.2σ after considering the systematic uncertainties. The ratio of the branching fraction of $\Omega_c^0 \to \pi^+\Omega(2012)^- \to \pi^+(\bar{K}\Xi)^-$ relative to that of $\Omega_c^0 \to \pi^+\Omega^-$ is calculated to be $0.220 \pm 0.059(\text{stat.}) \pm 0.035(\text{syst.})$. The individual ratios of the branching fractions of the two isospin modes are also determined and found to be $\mathcal{B}(\Omega_c^0 \to \pi^+\Omega(2012)^-) \times \mathcal{B}(\Omega(2012)^- \to K^-\Xi^0)/\mathcal{B}(\Omega_c^0 \to \pi^+K^-\Xi^0) = (9.6 \pm 3.2(\text{stat.}) \pm 1.8(\text{syst.}))\%$ and $\mathcal{B}(\Omega_c^0 \to \pi^+\Omega(2012)^-) \times \mathcal{B}(\Omega(2012)^- \to \bar{K}^0\Xi^-)/\mathcal{B}(\Omega_c^0 \to \pi^+\bar{K}^0\Xi^-) = (5.5 \pm 2.8(\text{stat.}) \pm 0.7(\text{syst.}))\%$.

DOI: 10.1103/PhysRevD.104.052005

Several excited Ω^- baryons have been observed [1]; the latest addition was an excited Ω^- state decaying into $K^-\Xi^0$ and $K_S^0\Xi^-$ observed by Belle in 2018 using data samples collected at the $\Upsilon(1S)$, $\Upsilon(2S)$, and $\Upsilon(3S)$ resonances [2]. This new excited Ω^- state is called the $\Omega(2012)^-$ and has a measured mass of $(2012.4 \pm 0.7(\text{stat.}) \pm 0.6(\text{syst.}))$ MeV/c^2 and width of $(6.4^{+2.5}_{-2.0}(\text{stat.}) \pm 1.6(\text{syst.}))$ MeV.

Following the discovery of the $\Omega(2012)^-$, several interpretations of the state were suggested [3–9]. The mass and the two-body strong decays of the $\Omega(2012)^-$ were studied in the framework of quantum chromodynamics sum rules [3,4], and this showed that the $\Omega(2012)^-$ could be interpreted as a $1P$ orbital excitation of the ground-state Ω^- baryon with a spin-parity $J^P = 3/2^-$. As the mass of the $\Omega(2012)^-$ is very close to the $(\bar{K}\Xi(1530))^-$ threshold, it was interpreted as a $(\bar{K}\Xi(1530))^-$ hadronic molecule in Refs. [5–9]. These hadronic molecule models predicted a large decay width for $\Omega(2012)^- \to (\bar{K}\pi\Xi)^-$.

The three-body decay $\Omega(2012)^- \to (\bar{K}\Xi(1530))^- \to (\bar{K}\pi\Xi)^-$ has been searched for by Belle [10]. No significant signals were found for the $\Omega(2012)^- \to (\bar{K}\Xi(1530))^- \to (\bar{K}\pi\Xi)^-$ decay, and the 90% credibility level (C.L.) upper limit on the ratio of $\mathcal{R}^{(\bar{K}\pi\Xi)^-}_{(\bar{K}\Xi)^-} = \mathcal{B}(\Omega(2012)^- \to (\bar{K}\Xi(1530))^- \to (\bar{K}\pi\Xi)^-)/\mathcal{B}(\Omega(2012)^- \to (\bar{K}\Xi)^-)$ was determined to be 0.119. Based on this upper limit for the ratio $\mathcal{R}^{(\bar{K}\pi\Xi)^-}_{(\bar{K}\Xi)^-}$, the authors in Refs. [11,12] revisited the $\Omega(2012)^-$ resonance from the molecular perspective and concluded that the experimental data were still consistent with their molecular picture with a certain set of naturally allowed parameters. On the other hand, the authors of Ref. [13] conducted a dynamical calculation of pentaquark systems with quark contents $sssu\bar{u}$ in the framework of the chiral quark model [14] and the quark delocalization color screening model [15,16], and concluded that the $\Omega(2012)^-$ is not suitable to be interpreted as a $(\bar{K}\Xi(1530))^-$ molecular state.

A theoretical study of the $\Omega(2012)^-$ resonance in the nonleptonic weak decays $\Omega_c^0 \to \pi^+\bar{K}\Xi(1530)(\eta\Omega) \to \pi^+(\bar{K}\pi\Xi)^-$ and $\pi^+(\bar{K}\Xi)^-$ via final-state interactions of the $\bar{K}\Xi(1530)$ and $\eta\Omega$ pairs has been reported [17]. The authors found that the $\Omega_c^0 \to \pi^+(\bar{K}\pi\Xi)^-$ decay is not well suited to study the $\Omega(2012)^-$ because the dominant contribution is from the $\Omega_c^0 \to \pi^+(\bar{K}\Xi(1530))^-$ decay at tree level, and this will not contribute to the production of the $\Omega(2012)^-$. On the other hand, they predicted that the $\Omega(2012)^-$ would be visible in the $(\bar{K}\Xi)^-$ invariant mass spectrum of the $\Omega_c^0 \to \pi^+(\bar{K}\Xi)^-$ decay. It is clear that observing the $\Omega(2012)^-$ in different production mechanisms can not only further confirm its existence but also yield important information that can increase the understanding of its internal structure.

In this paper, we search for the $\Omega(2012)^-$ in the decay $\Omega_c^0 \to \pi^+\Omega(2012)^- \to \pi^+(\bar{K}\Xi)^-$. We first perform the analysis separately for the two isospin modes ($\Omega_c^0 \to \pi^+\Omega(2012)^- \to \pi^+K^-\Xi^0/\pi^+K_S^0\Xi^-$) and then combine them for further analysis. Throughout this paper inclusion of charge-conjugate modes are implicitly assumed.

This analysis is based on data collected at or near the $\Upsilon(1S)$, $\Upsilon(2S)$, $\Upsilon(3S)$, $\Upsilon(4S)$, and $\Upsilon(5S)$ resonances by the Belle detector [18,19] at the KEKB asymmetric-energy e^+e^- collider [20,21]. The total data sample corresponds to an integrated luminosity of 980 fb^{-1} [19]. The Belle detector was a large-solid-angle magnetic spectrometer

consisting of a silicon vertex detector, a 50-layer central drift chamber (CDC), an array of aerogel threshold Cherenkov counters (ACC), a barrellike arrangement of time-of-flight scintillation counters (TOF), and an electromagnetic calorimeter comprising CsI(TI) crystals (ECL) located inside a superconducting solenoid coil that provides a $1.5T$ magnetic field. An iron flux return comprising resistive plate chambers located outside the coil was instrumented to detect K_L^0 mesons and to identify muons. A detailed description of the Belle detector can be found in Refs. [18,19].

Monte Carlo (MC) simulated signal events are generated using EvtGen [22] to optimize the signal selection criteria and calculate the reconstruction efficiencies. $e^+e^- \to c\bar{c}$ events are simulated using PYTHIA [23], where one of the two charm quarks hadronizes into an Ω_c^0 baryon. Both $\Omega_c^0 \to \pi^+\Omega(2012)^-$ and $\Omega(2012)^- \to K^-\Xi^0/K_S^0\Xi^-$ decays are isotropic in the rest frame of the parent particle. We also generate the signal MC events of $\Omega_c^0 \to \pi^+K^-\Xi^0/\pi^+K_S^0\Xi^-$ decays with a phase-space model to estimate the reconstruction efficiencies of the reference modes. The simulated events are processed with a detector simulation based on GEANT3 [24]. Inclusive MC samples of $\Upsilon(1S, 2S, 3S)$ decays, $\Upsilon(4S) \to B^+B^-/B^0\bar{B}^0$, $\Upsilon(5S) \to B_{(s)}^{(*)}\bar{B}_{(s)}^{(*)}$, and $e^+e^- \to q\bar{q}$ ($q = u, d, s, c$) at center-of-mass (C.M.) energies of 10.520, 10.580, and 10.867 GeV corresponding to 4 times the integrated luminosity of data are used to optimize the signal selection criteria and to check possible peaking backgrounds [25].

The impact parameters of the charged particle tracks, except for those of the decay products of K_S^0, Λ, and Ξ^-, measured with respect to the nominal interaction point (IP), are required to be less than 0.2 cm perpendicular to the beam direction and less than 1 cm parallel to it. For the particle identification (PID) of a well-reconstructed charged track, information from different detector subsystems, including specific ionization in the CDC, time measurement in the TOF, and the response of the ACC, is combined to form a likelihood $\mathcal{L}_i$ [26] for particle species i, where $i = K$, π, or p. Kaon candidates are defined as those with $\mathcal{L}_K/(\mathcal{L}_K + \mathcal{L}_p) > 0.8$ and $\mathcal{L}_K/(\mathcal{L}_K + \mathcal{L}_\pi) > 0.8$, which is approximately 87% efficient. For protons the requirements are $\mathcal{L}_p/(\mathcal{L}_p + \mathcal{L}_K) > 0.2$ and $\mathcal{L}_p/(\mathcal{L}_p + \mathcal{L}_\pi) > 0.2$, while for charged pions $\mathcal{L}_\pi/(\mathcal{L}_\pi + \mathcal{L}_K) > 0.2$ and $\mathcal{L}_\pi/(\mathcal{L}_\pi + \mathcal{L}_p) > 0.2$; these requirements are approximately 99% efficient.

An ECL cluster is taken as a photon candidate if it does not match the extrapolation of any charged track. The π^0 candidates are reconstructed from two photons having energy exceeding 30 MeV in the barrel or 50 MeV in the end caps. The reconstructed invariant mass of the π^0 candidate is required to be within 10.8 MeV/c^2 of the π^0 nominal mass [1], corresponding to approximately twice the resolution (σ). To reduce the large combinatorial backgrounds, the momentum of the π^0 candidate is required to exceed 200 MeV/c [2]. Λ candidates are reconstructed from $p\pi^-$ pairs with a production vertex significantly separated from the IP, and a reconstructed invariant mass within 3.5 MeV/c^2 of the Λ nominal mass [1] ($\sim 3\sigma$).

The $\Xi^0 \to \Lambda\pi^0$ reconstruction is performed as follows. The selected Λ candidate is combined with a π^0 to form a Ξ^0 candidate, and then taking the IP as the point of origin of the Ξ^0, the sum of the Λ and π^0 momenta is taken as the momentum vector of the Ξ^0 candidate. The intersection of this trajectory with the reconstructed Λ trajectory is then found, and this position is taken as the decay location of the Ξ^0 baryon. The π^0 is then refit using this location as its point of origin. Only those combinations with the decay location of the Ξ^0 indicating a positive Ξ^0 path length of greater than 2 cm but less than the distance between the Λ decay vertex and the IP are retained [2]. The Ξ^- candidate is reconstructed by combining a Λ candidate with a π^-. The vertex formed from the Λ and π^- is required to be at least 0.35 cm from the IP, to have a shorter distance from the IP than the Λ decay vertex, and to signify a positive Ξ^- flight distance [2].

The K_S^0 candidates are first reconstructed from pairs of oppositely charged tracks, which are treated as pions, with a production vertex significantly separated from the average IP, and then selected using an artificial neural network [27] based on two sets of input variables [28].

The Ξ^0 and Ξ^- are kinematically constrained to their nominal masses [1], and then combined with a K^- or K_S^0 to form an $\Omega(2012)^-$ candidate. Finally, the reconstructed $\Omega(2012)^-$ candidate is combined with a π^+ to form an Ω_c^0 candidate. To improve the momentum resolution and suppress the backgrounds, a vertex fit (the IP is not included in this vertex) is performed for the $\pi^+(\bar{K}\Xi)^-$ final state, and then $\chi^2_{\text{vertex}} < 20$ is required, corresponding to an efficiency exceeding 90%.

To reduce combinatorial backgrounds, especially from B-meson decays, the scaled momentum $x_p = p^*_{\Omega_c^0}/p_{\max}$ is required to be larger than 0.6. Here, $p^*_{\Omega_c^0}$ is the momentum of Ω_c^0 candidates in the e^+e^- C.M. frame, and $p_{\max} = \sqrt{E^2_{\text{beam}} - M^2_{\Omega_c^0}c^4}/c$, where E_{beam} is the beam energy in the e^+e^- C.M. frame and $M_{\Omega_c^0}$ is the invariant mass of Ω_c^0 candidates. This criterion is optimized by maximizing the Punzi figure of merit = $S/(3/2 + \sqrt{B})$ [29], where S is the number of expected $\Omega_c^0 \to \pi^+\Omega(2012)^- \to \pi^+(\bar{K}\Xi)^-$ signal events from signal MC samples, by performing a two-dimensional (2D) maximum-likelihood fit to $M((\bar{K}\Xi)^-)$ and $M(\pi^+\Omega(2012)^-)$ distributions and assuming $\sigma(e^+e^- \to \Omega_c^0 + \text{anything}) \times \mathcal{B}(\Omega_c^0 \to \pi^+\Omega(2012)^-) \times \mathcal{B}(\Omega(2012)^- \to (\bar{K}\Xi)^-) = 10$ fb, and B is the number of background events from a 2D fit from inclusive MC samples.

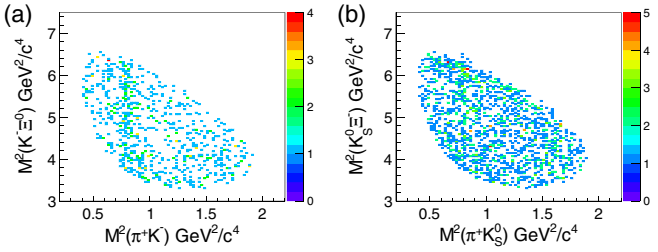

FIG. 1. The Dalitz plots of (a) $M^2(K^-\Xi^0)$ versus $M^2(\pi^+K^-)$ and (b) $M^2(K^0_S\Xi^-)$ versus $M^2(\pi^+K^0_S)$ from selected $\Omega_c^0 \to \pi^+K^-\Xi^0$ and $\Omega_c^0 \to \pi^+K^0_S\Xi^-$ candidates.

Reconstructed invariant masses for Ξ^0, K^0_S, and Ξ^- candidates are required to be within 7.0, 7.0, and 3.5 MeV/c^2 of the corresponding nominal masses [1] ($> 94\%$ signal events are retained for each intermediate state), respectively. These requirements are optimized using the same method as was used for scaled momentum.

Finally, if there are multiple Ω_c^0 candidates in an event, all the combinations are retained for further analysis. The fractions of events with multiple combinations for $\Omega_c^0 \to \pi^+\Omega(2012)^- \to \pi^+K^-\Xi^0$ and $\Omega_c^0 \to \pi^+\Omega(2012)^- \to \pi^+K^0_S\Xi^-$ decays are 2.4% and 0.8%, respectively, which are consistent with the signal MC expectations.

After applying the aforementioned event selection criteria, the Dalitz plots of $M^2(K^-\Xi^0)$ versus $M^2(\pi^+K^-)$ and $M^2(K^0_S\Xi^-)$ versus $M^2(\pi^+K^0_S)$ in the Ω_c^0 signal region are shown in Fig. 1, where the reconstructed invariant mass of Ω_c^0 candidates is required to be within 15 MeV/c^2 of the Ω_c^0 nominal mass [1] ($\sim 2.5\sigma$).

To extract the $\Omega(2012)^-$ signal events from Ω_c^0 decay, we perform a 2D unbinned maximum-likelihood fit to $M(K^-\Xi^0)/M(K^0_S\Xi^-)$ and $M(\pi^+\Omega(2012)^-)$ distributions. The 2D fitting function $f(M_1, M_2)$ is expressed as

$$f(M_1,M_2) = N_{\rm ss}^{\rm sig} s_1(M_1)s_2(M_2) + N_{\rm sb}^{\rm bg} s_1(M_1)b_2(M_2) + N_{\rm bs}^{\rm bg} b_1(M_1)s_2(M_2) + N_{\rm bb}^{\rm bg} b_1(M_1)b_2(M_2),$$

where $s_1(M_1)$ and $b_1(M_1)$ are the signal and background probability density functions (PDFs) for the $M(K^-\Xi^0)/M(K^0_S\Xi^-)$ distributions, respectively, and $s_2(M_2)$ and $b_2(M_2)$ are the corresponding PDFs for the $M(\pi^+\Omega(2012)^-)$ distributions. Here, $N_{\rm ss}^{\rm sig}$ is the number of signal events, $N_{\rm sb}^{\rm bg}$ and $N_{\rm bs}^{\rm bg}$ denote the numbers of peaking background events in $M(K^-\Xi^0)/M(K^0_S\Xi^-)$ and $M(\pi^+\Omega(2012)^-)$ distributions, respectively, and $N_{\rm bb}^{\rm bg}$ is the number of combinatorial background events both for $\Omega(2012)^-$ and Ω_c^0 candidates. The signal shapes [$s_1(M_1)$ and $s_2(M_2)$] of $\Omega(2012)^-$ and Ω_c^0 candidates are described by a Breit-Wigner (BW) function convolved with a Gaussian function and a double-Gaussian function, respectively, and first-order polynomial functions represent the backgrounds

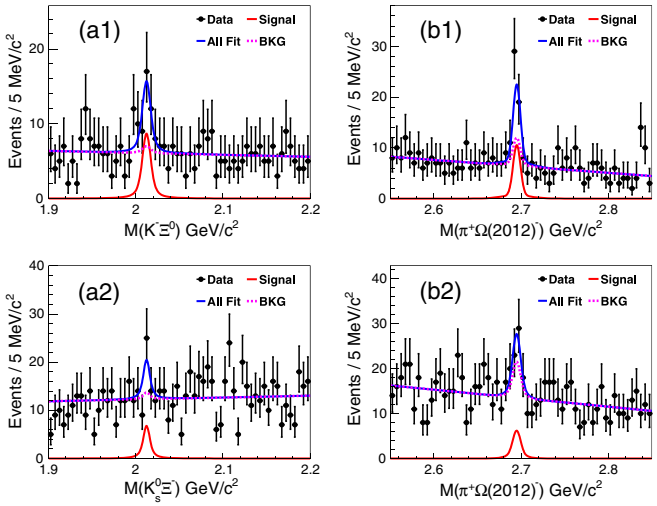

FIG. 2. The 1D projections of the 2D fits of (a) $M(K^-\Xi^0)/M(K^0_S\Xi^-)$ and (b) $M(\pi^+\Omega(2012)^-)$ distributions for (1) $\Omega_c^0 \to \pi^+\Omega(2012)^- \to \pi^+K^-\Xi^0$ and (2) $\Omega_c^0 \to \pi^+\Omega(2012)^- \to \pi^+K^0_S\Xi^-$ decays in data. All components are indicated in the legends and described in the text.

[$b_1(M_1)$ and $b_2(M_2)$]. The values of signal PDF parameters are fixed to those obtained from the fits to the corresponding simulated signal distributions. The values of the background shape parameters are allowed to float in the fit. The one-dimensional (1D) projections of $M(K^-\Xi^0)/M(K^0_S\Xi^-)$ in the Ω_c^0 signal region and $M(\pi^+\Omega(2012)^-)$ in the $\Omega(2012)^-$ signal region from 2D fits are shown in Fig. 2. The signal regions of $\Omega(2012)^-$ and Ω_c^0 candidates are defined as $|M(K^-\Xi^0)/M(K^0_S\Xi^-) - m(\Omega(2012)^-)| < 20$ MeV/c^2 ($\sim 2.5\sigma$) and $|M(\pi^+\Omega(2012)^-) - m(\Omega_c^0)| < 15$ MeV/c^2 ($\sim 2.5\sigma$), respectively, where $m(\Omega(2012)^-)$ and $m(\Omega_c^0)$ are the nominal masses of $\Omega(2012)^-$ and Ω_c^0 [1]. The numbers of fitted $\Omega_c^0 \to \pi^+\Omega(2012)^- \to \pi^+K^-\Xi^0$ and $\Omega_c^0 \to \pi^+\Omega(2012)^- \to \pi^+K^0_S\Xi^-$ signal events are 28.3 ± 8.9 and 17.9 ± 8.9 with statistical significances of 4.0σ and 2.3σ, respectively. Here, the statistical significances are defined as $\sqrt{-2\ln(\mathcal{L}_0/\mathcal{L}_{\rm max})}$, where $\mathcal{L}_0$ and $\mathcal{L}_{\rm max}$ are the maximized likelihoods without and with a signal component, respectively.

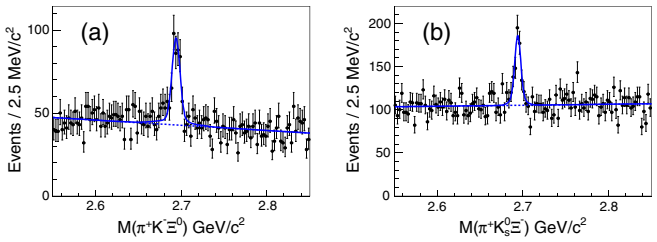

FIG. 3. The (a) $M(\pi^+K^-\Xi^0)$ and (b) $M(\pi^+K^0_S\Xi^-)$ distributions in data. The blue solid curves show the best-fit results, and the blue dashed curves show the fitted backgrounds.

For $\Omega_c^0 \to \pi^+ K^- \Xi^0$ and $\Omega_c^0 \to \pi^+ K_S^0 \Xi^-$ decays, the $M(\pi^+ K^- \Xi^0)$ and $M(\pi^+ K_S^0 \Xi^-)$ distributions are shown in Fig. 3, together with the fitted results. The signal shapes of Ω_c^0 are described by double-Gaussian functions, where the parameters are fixed to those obtained from the fits to the corresponding simulated signal distributions. The backgrounds are parametrized by first-order polynomial functions. The fitted $\Omega_c^0 \to \pi^+ K^- \Xi^0$ and $\Omega_c^0 \to \pi^+ K_S^0 \Xi^-$ signal yields are 279 ± 27 and 317 ± 32, respectively.

The branching fraction ratios are calculated according to the formulas,

$$\begin{aligned}\mathcal{R}_1 &= \frac{\mathcal{B}(\Omega_c^0 \to \pi^+ \Omega(2012)^-)\mathcal{B}(\Omega(2012)^- \to K^- \Xi^0)}{\mathcal{B}(\Omega_c^0 \to \pi^+ K^- \Xi^0)} \\ &= \frac{N^{\rm obs}_{\pi^+\Omega(2012)^-(\to K^-\Xi^0)} \times \epsilon_{\pi^+ K^- \Xi^0}}{N^{\rm obs}_{\pi^+ K^- \Xi^0} \times \epsilon_{\pi^+\Omega(2012)^-(\to K^-\Xi^0)}} \\ &= (9.6 \pm 3.2(\text{stat.}) \pm 1.8(\text{syst.}))\%,\end{aligned}$$

and

$$\begin{aligned}\mathcal{R}_2 &= \frac{\mathcal{B}(\Omega_c^0 \to \pi^+ \Omega(2012)^-)\mathcal{B}(\Omega(2012)^- \to \bar{K}^0 \Xi^-)}{\mathcal{B}(\Omega_c^0 \to \pi^+ \bar{K}^0 \Xi^-)} \\ &= \frac{N^{\rm obs}_{\pi^+\Omega(2012)^-(\to K_S^0\Xi^-)} \times \epsilon_{\pi^+ K_S^0 \Xi^-}}{N^{\rm obs}_{\pi^+ K_S^0 \Xi^-} \times \epsilon_{\pi^+\Omega(2012)^-(\to K_S^0\Xi^-)}} \\ &= (5.5 \pm 2.8(\text{stat.}) \pm 0.7(\text{syst.}))\%.\end{aligned}$$

Here, $N^{\rm obs}_{\pi^+\Omega(2012)^-(\to K^-\Xi^0)}$, $N^{\rm obs}_{\pi^+\Omega(2012)^-(\to K_S^0\Xi^-)}$, $N^{\rm obs}_{\pi^+ K^- \Xi^0}$, and $N^{\rm obs}_{\pi^+ K_S^0 \Xi^-}$ are the fitted signal yields in the decay modes $\Omega_c^0 \to \pi^+ \Omega(2012)^- \to \pi^+ K^- \Xi^0$, $\Omega_c^0 \to \pi^+ \Omega(2012)^- \to \pi^+ K_S^0 \Xi^-$, $\Omega_c^0 \to \pi^+ K^- \Xi^0$, and $\Omega_c^0 \to \pi^+ K_S^0 \Xi^-$, respectively; $\epsilon_{\pi^+\Omega(2012)^-(\to K^-\Xi^0)}$, $\epsilon_{\pi^+\Omega(2012)^-(\to K_S^0\Xi^-)}$, $\epsilon_{\pi^+ K^- \Xi^0}$, and $\epsilon_{\pi^+ K_S^0 \Xi^-}$ are the corresponding reconstruction efficiencies, which are obtained from the signal MC simulations and are listed in Table I. The systematic uncertainties are discussed below.

From these fitted signal yields and reconstruction efficiencies, and the intermediate state branching fractions of $\Omega_c^0 \to \pi^+ \Omega(2012)^- \to \pi^+ K^- \Xi^0$ and $\Omega_c^0 \to \pi^+ \Omega(2012)^- \to \pi^+ K_S^0 \Xi^-$ decays [1], the branching fraction ratio $\mathcal{B}(\Omega(2012)^- \to K^- \Xi^0)/\mathcal{B}(\Omega(2012)^- \to \bar{K}^0 \Xi^-)$ is determined to be $1.19 \pm 0.70(\text{stat.})$, which is consistent with the expectation of isospin symmetry and the previously measured value of 1.2 ± 0.3 by Belle [2].

TABLE I. Summary of the fitted signal yields ($N^{\rm obs}$) and reconstruction efficiencies (ϵ). All the uncertainties here are statistical only.

Mode	$N^{\rm obs}$	$\epsilon(\%)$
$\Omega_c^0 \to \pi^+ \Omega(2012)^- \to \pi^+ K^- \Xi^0$	28.3 ± 8.9	3.59
$\Omega_c^0 \to \pi^+ \Omega(2012)^- \to \pi^+ K_S^0 \Xi^-$	17.9 ± 8.9	7.68
$\Omega_c^0 \to \pi^+ K^- \Xi^0$	279 ± 27	3.41
$\Omega_c^0 \to \pi^+ K_S^0 \Xi^-$	317 ± 32	7.41

Assuming $\mathcal{B}(\Omega(2012)^- \to K^- \Xi^0) = \mathcal{B}(\Omega(2012)^- \to \bar{K}^0 \Xi^-)$ based on isospin symmetry, the ratio of the expected signal yields of $\Omega_c^0 \to \pi^+ \Omega(2012)^- \to \pi^+ K^- \Xi^0$ and $\Omega_c^0 \to \pi^+ \Omega(2012)^- \to \pi^+ K_S^0 \Xi^-$ decays is 57.1%:42.9% after considering the products of detection efficiency and intermediate-state branching fractions $\epsilon_i \mathcal{B}_i$ ($i = 1, 2$), where ϵ_1 and ϵ_2 are the corresponding detection efficiencies, $\mathcal{B}_1 = \mathcal{B}(\Xi^0 \to \Lambda \pi^0) \times \mathcal{B}(\pi^0 \to \gamma\gamma)$, and $\mathcal{B}_2 = \mathcal{B}(\Xi^- \to \Lambda \pi^-) \times \mathcal{B}(\bar{K}^0 \to K_S^0) \times \mathcal{B}(K_S^0 \to \pi^+ \pi^-)$ [1]. We perform a 2D unbinned maximum-likelihood simultaneous fit to $M((\bar{K}\Xi)^-)$ and $M(\pi^+ \Omega(2012)^-)$ distributions, where the ratio of the expected signal yields of two isospin modes is fixed to 57.1%:42.9%, and the functions used to describe the signal and background shapes are parametrized as before. The 1D projections of $M((\bar{K}\Xi)^-)$ in the Ω_c^0 signal region and $M(\pi^+ \Omega(2012)^-)$ in the $\Omega(2012)^-$ signal region from the 2D simultaneous fit are shown in Fig. 4, corresponding to a total signal yield of 46.6 ± 12.3. The statistical significance of the $\Omega(2012)^-$ signal in $\Omega_c^0 \to \pi^+ \Omega(2012)^- \to \pi^+ (\bar{K}\Xi)^-$ decay is 4.6σ. The fitting ranges and background shapes are the dominant systematic uncertainties for the estimate of the signal significance. If the background shapes are replaced by second-order polynomial functions and fitting ranges are changed, the $\Omega(2012)^-$ signal significance in the simultaneous fit is reduced to 4.2σ corresponding to a total signal yield of 44.7 ± 12.4. We take this value as the signal significance with systematic uncertainties included.

The $\Omega(2012)^-$ was first observed in data taken at the $\Upsilon(1S)$, $\Upsilon(2S)$, and $\Upsilon(3S)$ resonances [2]. In order to make a statistically independent check of its existence, we exclude these datasets from our sample and repeat the fitting procedure used to produce Fig. 4. The total number of signal events of $\Omega_c^0 \to \pi^+ \Omega(2012)^- \to \pi^+ (\bar{K}\Xi)^-$ is 38.9 ± 11.2 in this reduced data sample which corresponds to an integrated luminosity of 949.5 fb^{-1}, and the statistical significance of the signal is 4.2σ. We prefer to use the entire

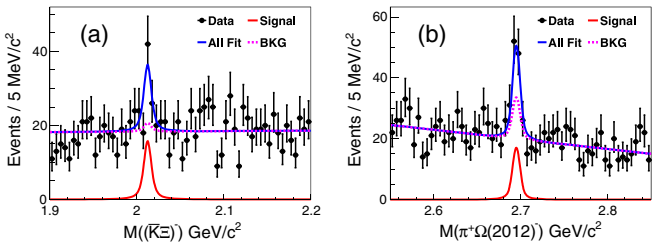

FIG. 4. The 1D projections of the 2D simultaneous fit of (a) $M((\bar{K}\Xi)^-)$ and (b) $M(\pi^+ \Omega(2012)^-)$ distributions in data. All components are indicated in the legends and described in the text.

TABLE II. Relative systematic uncertainties (%) on the measurements of $\mathcal{R}_1$, $\mathcal{R}_2$, and $\mathcal{R}_3$.

Sources	$\mathcal{R}_1$	$\mathcal{R}_2$	$\mathcal{R}_3$
Detection-efficiency-related	...	...	2.2
MC statistics	1.0	1.0	1.0
$\Omega(2012)$ resonance parameters	14.3	9.2	12.8
Ξ^0 mass	4.2	...	3.2
Fit	10.4	9.9	7.8
Ratio	...	...	2.3
Sum in quadrature	18.2	13.6	15.7

dataset for our investigation of the branching fractions of the Ω_c^0.

The ratio of the branching fraction of $\Omega_c^0 \to \pi^+\Omega(2012)^- \to \pi^+(\bar{K}\Xi)^-$ relative to that of $\Omega_c^0 \to \pi^+\Omega^-$ decay is also calculated from the following formula:

$$\begin{aligned}\mathcal{R}_3 &= \frac{\mathcal{B}(\Omega_c^0 \to \pi^+\Omega(2012)^-) \times \mathcal{B}(\Omega(2012)^- \to (\bar{K}\Xi)^-)}{\mathcal{B}(\Omega_c^0 \to \pi^+\Omega^-)} \\ &= \frac{N^{\rm obs}_{\rm sig.} \times \epsilon_{\pi^+\Omega^-}}{N^{\rm obs}_{\pi^+\Omega^-} \times (f_1 \times \epsilon_1 \times \mathcal{B}_1 + f_2 \times \epsilon_2 \times \mathcal{B}_2)} \\ &= 0.220 \pm 0.059(\text{stat.}) \pm 0.035(\text{syst.}),\end{aligned}$$

where $N^{\rm obs}_{\rm sig.}$ is the fitted signal yield from the simultaneous fit in the decay $\Omega_c^0 \to \pi^+\Omega(2012)^- \to \pi^+(\bar{K}\Xi)^-$; ϵ_1 and ϵ_2 are the corresponding reconstruction efficiencies from the signal MC simulations; according to isospin symmetry, $f_1 = \mathcal{B}(\Omega(2012)^- \to K^-\Xi^0)/\mathcal{B}(\Omega(2012)^- \to (\bar{K}\Xi)^-) = 0.5$, $f_2 = \mathcal{B}(\Omega(2012)^- \to \bar{K}^0\Xi^-)/\mathcal{B}(\Omega(2012)^- \to (\bar{K}\Xi)^-) = 0.5$; $\mathcal{B}_1$ and $\mathcal{B}_2$ are the corresponding products of secondary branching fractions defined above; $N^{\rm obs}_{\pi^+\Omega^-} = 691 \pm 29$ and $\epsilon_{\pi^+\Omega^-} = 10.08\%$ are the number of signal events and detection efficiency of $\Omega_c^0 \to \pi^+\Omega^-$ decay taken from Ref. [30].

There are several sources of systematic uncertainties for the measurements of branching fraction ratios $\mathcal{R}_1$, $\mathcal{R}_2$, and $\mathcal{R}_3$ as listed in Table II, including detection-efficiency-related uncertainties, the statistical uncertainty of the MC efficiency, the modeling of MC event generation, the branching fractions of intermediate states, the $\Omega(2012)^-$ resonance parameters, the uncertainty in the Ξ^0 mass (as evaluated from the difference between the reconstructed value and the world average value) as well as the overall fit uncertainty.

The detection-efficiency-related uncertainties include those for tracking efficiency (0.35% per track), PID efficiency (1.2% per kaon, 1.0% or 1.2% per pion depending on the specific decay mode), K_S^0 selection efficiency (1.7%), as well as π^0 reconstruction efficiency (2.25%). For the measurements of $\mathcal{R}_1$ and $\mathcal{R}_2$, the detection-efficiency-related sources can cancel. For the measurement of $\mathcal{R}_3$, the common sources of systematic uncertainties such as Λ selection cancel; to determine the total detection-efficiency-related uncertainties, the above individual uncertainties from different reconstructed modes ($\sigma_{i/\pi^+\Omega^-}$) are added using the following standard error propagation formula

$$\sigma^{\mathcal{R}_3}_{\rm DER} = \sqrt{\frac{\Sigma_i(\mathcal{W}_i \times \sigma_i)^2}{(\Sigma_i \mathcal{W}_i)^2} + \sigma^2_{\pi^+\Omega^-}},$$

where $\mathcal{W}_i$ ($\mathcal{W}_1 = f_1 \times \epsilon_1 \times \mathcal{B}_1$, $\mathcal{W}_2 = f_2 \times \epsilon_2 \times \mathcal{B}_2$) is the weight factor for the ith ($i = 1, 2$) mode of $\Omega_c^0 \to \pi^+\Omega(2012)^- \to \pi^+(\bar{K}\Xi)^-$ decays. Assuming these sources are independent and adding them in quadrature, the final uncertainty related to the reconstruction efficiency in the measurement of $\mathcal{R}_3$ is 2.2%.

The MC statistical uncertainties are all 1.0% or less. We assume that both $\Omega_c^0 \to \pi^+\Omega(2012)^-$ and $\Omega(2012)^- \to K^-\Xi^0/K_S^0\Xi^-$ decays are isotropic in the rest frame of the parent particle, and a phase space model is used to generate signal events. Since the signal efficiency is independent of the decay angular distributions of π^+ in Ω_c^0 C.M. and K^-/K_S^0 in $\Omega(2012)^-$ C.M., the model-dependent uncertainty has negligible effect on efficiency. For the measurement of $\mathcal{R}_3$, the uncertainties from the $\mathcal{B}(\Xi^0 \to \Lambda\pi^0)$, $\mathcal{B}(\Xi^- \to \Lambda\pi^-)$, $\mathcal{B}(K_S^0 \to \pi^+\pi^-)$, and $\mathcal{B}(\pi^0 \to \gamma\gamma)$ are 0.012%, 0.035%, 0.072%, and 0.035% [1], respectively, which are small and neglected. The uncertainties related to the mass and width of $\Omega(2012)^-$ resonance are considered as different sources and are estimated by changing the values of resonance mass and width by $\pm 1\sigma$ and refitting [2]. The largest differences compared to the nominal fit results are added in quadrature as systematic uncertainty. The uncertainty in the Ξ^0 mass is estimated by comparing the signal yields of $\Omega_c^0 \to \pi^+\Omega(2012)^- \to \pi^+K^-\Xi^0/\pi^+(\bar{K}\Xi)^-$ for the case where the reconstructed Ξ^0 mass is fixed at the found peak value versus the case where the mass is fixed at the nominal mass [1].

The systematic uncertainties associated with the fit range, background shape, and mass resolution are considered as follows. To consider the uncertainty due to mass resolution, we enlarge the mass resolution of signal by 10% and take the difference in the number of signal events as the systematic uncertainty. The order of the background polynomial is replaced by a higher-order Chebyshev function and the fit range is changed. The largest deviation compared to the nominal fit results is taken as the systematic uncertainty. For each mode, all the above uncertainties are summed in quadrature to obtain the total systematic uncertainty due to the fit. Finally, the fit uncertainties of signal and reference modes are added in quadrature as total fit uncertainties in the measurements of branching fraction ratios.

We estimate the uncertainty in $\mathcal{R}_3$ associated with the ratio of the expected signal yields of the $\Omega_c^0 \to \pi^+\Omega(2012)^- \to \pi^+K^-\Xi^0$ and $\Omega_c^0 \to \pi^+\Omega(2012)^- \to \pi^+K_S^0\Xi^-$ decays by constraining the ratio of

$\mathcal{B}(\Omega(2012)^- \to K^-\Xi^0)$:$\mathcal{B}(\Omega(2012)^- \to \bar{K}^0\Xi^-)$ to 1.2:1 [2] rather than taking the value of 1:1 which assumes exact isospin symmetry. The resultant change in $\mathcal{R}_3$ is 2.3%, which is taken as the systematic uncertainty.

Assuming all the sources are independent and adding them in quadrature, the total systematic uncertainties are obtained. All the systematical uncertainties are summarized in Table II.

In summary, using the entire data sample of 980 fb^{-1} integrated luminosity collected with the Belle detector, we search for the $\Omega(2012)^-$ resonance in $\Omega_c^0 \to \pi^+\Omega(2012)^- \to \pi^+(\bar{K}\Xi)^-$. In $\Omega_c^0 \to \pi^+\Omega(2012)^- \to \pi^+K^-\Xi^0$, we find evidence for the $\Omega(2012)^-$ in the $K^-\Xi^0$ invariant mass spectrum with a statistical significance of 4.0σ. In $\Omega_c^0 \to \pi^+\Omega(2012)^- \to \pi^+K_S^0\Xi^-$, a marginal $\Omega(2012)^-$ signal can be seen in the $K_S^0\Xi^-$ invariant mass spectrum with a statistical significance of 2.3σ. We perform a 2D simultaneous fit to the two isospin decay modes, and the significance of $\Omega(2012)^-$ in $\Omega_c^0 \to \pi^+\Omega(2012)^- \to \pi^+(\bar{K}\Xi)^-$ is 4.2σ, including the systematic uncertainties. The ratios of the branching fractions $\mathcal{B}(\Omega_c^0 \to \pi^+\Omega(2012)^-) \times \mathcal{B}(\Omega(2012)^- \to K^-\Xi^0)/\mathcal{B}(\Omega_c^0 \to \pi^+K^-\Xi^0)$, $\mathcal{B}(\Omega_c^0 \to \pi^+\Omega(2012)^-) \times \mathcal{B}(\Omega(2012)^- \to \bar{K}^0\Xi^-)/\mathcal{B}(\Omega_c^0 \to \pi^+\bar{K}^0\Xi^-)$, and $\mathcal{B}(\Omega_c^0 \to \pi^+\Omega(2012)^-) \times \mathcal{B}(\Omega(2012)^- \to (\bar{K}\Xi)^-)/\mathcal{B}(\Omega_c^0 \to \pi^+\Omega^-)$ are measured to be $(9.6 \pm 3.2(\text{stat.}) \pm 1.8(\text{syst.}))\%$, $(5.5 \pm 2.8(\text{stat.}) \pm 0.7(\text{syst.}))\%$, and $0.220 \pm 0.059(\text{stat.}) \pm 0.035(\text{syst.})$, respectively.

We thank the KEKB group for the excellent operation of the accelerator; the KEK cryogenics group for the efficient operation of the solenoid; and the KEK computer group, and the Pacific Northwest National Laboratory (PNNL) Environmental Molecular Sciences Laboratory (EMSL) computing group for strong computing support; and the National Institute of Informatics, and Science Information NETwork 5 (SINET5) for valuable network support. We acknowledge support from the Ministry of Education, Culture, Sports, Science, and Technology (MEXT) of Japan, the Japan Society for the Promotion of Science (JSPS), and the Tau-Lepton Physics Research Center of Nagoya University; the Australian Research Council including Grants No. DP180102629, No. DP170102389, No. DP170102204, No. DP150103061, No. FT130100303; Austrian Science Fund (FWF); the National Natural Science Foundation of China under Contracts No. 11435013, No. 11475187, No. 11521505, No. 11575017, No. 11675166, No. 11705209, No. 11761141009, No. 11975076, No. 12042509, No. 12135005; Key Research Program of Frontier Sciences, Chinese Academy of Sciences (CAS), Grant No. QYZDJ-SSW-SLH011; the CAS Center for Excellence in Particle Physics (CCEPP); the Shanghai Pujiang Program under Grant No. 18PJ1401000; the Ministry of Education, Youth and Sports of the Czech Republic under Contract No. LTT17020; the Carl Zeiss Foundation, the Deutsche Forschungsgemeinschaft, the Excellence Cluster Universe, and the VolkswagenStiftung; the Department of Science and Technology of India; the Istituto Nazionale di Fisica Nucleare of Italy; National Research Foundation (NRF) of Korea Grants No. 2016R1D1A1B01010135, No. 2016R1D1A1B02012900, No. 2018R1A2B3003643, No. 2018R1A6A1A06024970, No. 2018R1D1A1B07047294, No. 2019K1A3A7A09033840, No. 2019R1I1A3A01058933; Radiation Science Research Institute, Foreign Large-size Research Facility Application Supporting project, the Global Science Experimental Data Hub Center of the Korea Institute of Science and Technology Information and KREONET/GLORIAD; the Polish Ministry of Science and Higher Education and the National Science Center; the Ministry of Science and Higher Education of the Russian Federation, Agreement No. 14.W03.31.0026; the Slovenian Research Agency; Ikerbasque, Basque Foundation for Science, Spain; the Swiss National Science Foundation; the Ministry of Education and the Ministry of Science and Technology of Taiwan; and the United States Department of Energy and the National Science Foundation.

[1] P. A. Zyla *et al.* (Particle Data Group), Prog. Theor. Exp. Phys. **2020**, 083C01 (2020).
[2] J. Yelton *et al.* (Belle Collaboration), Phys. Rev. Lett. **121**, 052003 (2018).
[3] T. M. Aliev, K. Azizi, Y. Sarac, and H. Sundu, Phys. Rev. D **98**, 014031 (2018).
[4] T. M. Aliev, K. Azizi, Y. Sarac, and H. Sundu, Eur. Phys. J. C **78**, 894 (2018).
[5] Y. H. Lin and B. S. Zou, Phys. Rev. D **98**, 056013 (2018).
[6] M. P. Valderrama, Phys. Rev. D **98**, 054009 (2018).
[7] Y. Huang, M. Z. Liu, J. X. Lu, J. J. Xie, and L. S. Geng, Phys. Rev. D **98**, 076012 (2018).
[8] R. Pavao and E. Oset, Eur. Phys. J. C **78**, 857 (2018).
[9] M. V. Polyakov, H. D. Son, B. D. Sun, and A. Tandogan, Phys. Lett. B **792**, 315 (2019).
[10] S. Jia *et al.* (Belle Collaboration), Phys. Rev. D **100**, 032006 (2019).
[11] N. Ikeno, G. Toledo, and E. Oset, Phys. Rev. D **101**, 094016 (2020).

[12] J. X. Lu, C. H. Zeng, E. Wang, J. J. Xie, and L. S. Geng, Eur. Phys. J. C **80**, 361 (2020).
[13] X. J. Liu, H. X. Huang, J. L. Ping, and D. Y. Chen, Phys. Rev. C **103**, 025202 (2021).
[14] A. Valcarce, H. Garcilazo, F. Fernandez, and P. Gonzalez, Rep. Prog. Phys. **68**, 965 (2005) and references therein.
[15] F. Wang, G. H. Wu, L. J. Teng, and J. T. Goldman, Phys. Rev. Lett. **69**, 2901 (1992).
[16] G. H. Wu, J. L. Ping, L. J. Teng, F. Wang, and J. T. Goldman, Nucl. Phys. **A673**, 279 (2000).
[17] C. H. Zeng, J. X. Lu, E. Wang, J. J. Xie, and L. S. Geng, Phys. Rev. D **102**, 076009 (2020).
[18] A. Abashian *et al.* (Belle Collaboration), Nucl. Instrum. Methods Phys. Res., Sect. A **479**, 117 (2002).
[19] J. Brodzicka *et al.*, Prog. Theor. Exp. Phys. **2012**, 04D001 (2012).
[20] S. Kurokawa and E. Kikutani, Nucl. Instrum. Methods Phys. Res., Sect. A **499**, 1 (2003), and other papers included in this volume.
[21] T. Abe *et al.*, Prog. Theor. Exp. Phys. **2013**, 03A001 (2013), and references therein.
[22] D. J. Lange, Nucl. Instrum. Methods Phys. Res., Sect. A **462**, 152 (2001).
[23] T. Sjöstrand, P. Edén, C. Friberg, L. Lönnblad, G. Miu, S. Mrenna, and E. Norrbin, Comput. Phys. Commun. **135**, 238 (2001).
[24] R. Brun *et al.*, GEANT 3: User's guide Geant 3.10, Geant 3.11, CERN Report No. DD/EE/84-1, 1984.
[25] X. Y. Zhou, S. X. Du, G. Li, and C. P. Shen, Comput. Phys. Commun. **258**, 107540 (2021).
[26] E. Nakano, Nucl. Instrum. Methods Phys. Res., Sect. A **494**, 402 (2002).
[27] M. Feindt and U. Kerzel, Nucl. Instrum. Methods Phys. Res., Sect. A **559**, 190 (2006).
[28] H. Nakano, Ph.D. thesis, Tohoku University, 2014, Chapter 4, to be published, https://tohoku.repo.nii.ac.jp/?action=pages_view_main&active_action=repository_view_main_item_detail&item_id=70563&item_no=1&page_id=33&block_id=38.
[29] G. Punzi, eConf **C030908**, MODT002 (2003).
[30] J. Yelton *et al.* (Belle Collaboration), Phys. Rev. D **97**, 032001 (2018).